Available online at www.sciencedirect.com

ScienceDirect

Procedia Engineering 103 (2015) 458 – 465

Procedia Engineering

www.elsevier.com/locate/procedia

The 13th Hypervelocity Impact Symposium

Modeling Plastic Deformation of Steel Plates in Hypervelocity Impact Experiments

Brendan O'Toole[a*], Mohamed Trabia[a], Robert Hixson[b], Shawoon K. Roy[a], Michael Pena[b], Steven Becker[b], Edward Daykin[b], Eric Machorro[b], Richard Jennings[a], Melissa Matthes[a]

[a]*University of Nevada-Las Vegas, Las Vegas, NV 89119, USA*
[b]*National Security Technologies, LLC, Las Vegas, NV 89154, USA*

Abstract

Hypervelocity impact experiments were done with a two-stage light gas gun to study the plastic deformation of metallic plates. Cylindrical Lexan projectiles were fired at A36 steel target plates with a velocity range of 4.5-6.0 km/s. Experiments were designed to produce a front side impact crater and a permanent bulging deformation on the back surface of the target while preventing complete perforation. Free surface velocities from the back surface of target plate were acquired using the newly developed Multiplexed Photonic Doppler Velocimetry (MPDV) system. Two different computational techniques were developed to simulate this type of experiment: Lagrangian-based smooth particle hydrodynamics (SPH) in LS-DYNA and the Eulerian-based hydrocode CTH. Parameters for material models including equation of state, compressive strength, and spall model were selected to obtain highest fidelity numerical results to compare with experiment.

Peer-review under responsibility of the Curators of the University of Missouri On behalf of the Missouri University of Science and Technology

Keywords: Hypervelocity impact, Smooth Particle Hydrodynamics, CTH

1. Introduction

Hypervelocity impact research has been conducted using light gas guns over several decades for a wide variety of reasons; one of them is to characterize materials under shock conditions. In general, gas gun experiments produce high pressure and temperature states during the projectile-target interaction and shockwaves generated during such an impact event are similar to those found in micro-meteoritic collisions with spacecraft [1]. Projectile and target materials both experience severe localized deformation under these conditions, which creates stretching, bending, and complete perforation in thin target plates. On the other hand, thick target plates show several failure modes, such as spalling, petalling, discing, and plugging [2]. These failure modes are mostly controlled by several factors such as impact velocity, material properties, loading geometry etc.

In previous research, the perforation and deformation of thin steel plates at a velocity range of 3-9 km/s were studied and an analytical method was presented to relate debris particles to impact velocity [3]. A study of hypervelocity impact damage on martensitic steel armor highlighted the importance of better understanding spall

* Brendan O'Toole. Tel.: +1-702-895-3885 ; fax: +1-702-895-3936.
E-mail address: brendan.otoole@unlv.edu.

Peer-review under responsibility of the Curators of the University of Missouri On behalf of the Missouri University of Science and Technology
doi:10.1016/j.proeng.2015.04.060

damage and pressure-induced phase transitions [4]. Dynamic failure of SS400 steel under polycarbonate projectile impact was studied with a velocity up to 9 km/s and spall, pressure-induced α↔ε phase transition were discussed along with hydrocode simulation [5].

Most of the early experimental work in impact dynamics and shock physics were conducted with relatively simple diagnostic systems. Part of this was due to the complexity of the experiment and lack of sophisticated diagnostics technologies; these took decades to develop. Therefore, significant effort has taken place in the past few decades to develop new and accurate diagnostic systems to acquire data from this type of dynamic experiments. In many recent hypervelocity impact research, velocimetry based diagnostic systems provide insight in to dynamic yield strength, spall strength, Hugoniot elastic limit (HEL), and polymorphic phase transitions of materials. The Velocity Interferometer System for Any Reflector (VISAR) [6] was the first common velocimetry diagnostic tool developed for hypervelocity impact research. Ever since the introduction of VISAR, it became widely used in the shock physics community and numerous researchers listed VISAR as their primary diagnostic tool for dynamic impact experiments [7,8]. However, the complexity and cost of VISAR system prompted development of a more simple, and inexpensive diagnostic commonly called PDV (Photonic Doppler Velocimetry) [9]. One of the most important limitations of VISAR system was to resolve multiple velocity points. Therefore, developing a diagnostic tool which can resolve multiple velocity points was a demand from researchers at that time. The need of many channels of PDV on an experiment was addressed by introducing the concept of multiplexing with PDV systems [10,11]. Multiplexed PDV (MPDV) is one of the most powerful inventions in recent years and hence, gaining significant attention in dynamic experiments. Dynamic materials researchers are currently also focused on exploration of the abilities of MPDV systems, including accuracy, extraction analysis of MPDV data [12–16].

Many researchers have done numerical simulations of this kind of experiment using various computational techniques. We have worked to develop predictive computational models which will be accurate enough to simulate these experiments using two complementary numerical approaches. The accuracy of these computational models depend mostly on the use of appropriate shock physics models and input parameters [17]. Existing literature have already suggested using finite element analysis (FEA) software LS-DYNA as one of the computational tools to simulate this type of impact event [18,19]. This type of penetration problem produces relatively high pressure and temperature in both the impactor and target materials, so that use of a fluid mechanics or, hydrodynamic method of modeling the deformation is appropriate. Numerous literature papers listed Eulerian based hydrocode such as CTH to simulate different penetration problems in steel plates [20–22]. The Lagrangian-based smooth particle hydrodynamics (SPH) method is also listed as an alternative way to simulate this type impact penetration problem [23,24].

Despite a significant body of research done on various kind of steel plates subjected to hypervelocity impact conditions, only a few studies actually dealt with plastic deformation of plates instead of complete penetration. This work presents a unique approach in the use of an MPDV system to study plastic deformation of A36 steel [25].

2. Experimental Setup

A two-stage light gas gun (Fig. 1a) was used to perform all hypervelocity impact experiments. The propellant gas in powder breech drove a cylindrical piston into the pump tube. The moving piston then pressurized the light gas (hydrogen, helium, or nitrogen) in pump tube, which eventually burst a petal valve between the pump tube and the launch tube and accelerated the projectile down the launch tube and the drift tube. Projectile then impacted the target, which was bolted to a mounting frame inside the target chamber (Fig. 1b). An intervalometer system measured the projectile velocity by measuring the time interval between triggering two lasers at a specific locations in the drift tube.

All gas gun experiments performed in this work used Lexan projectiles, which were cylindrical rods of 5.58 mm diameter and 8.61 mm length. Targets were made of 152.4 x 152.4 x 12.7 mm ASTM A36 steel plates. The thickness of target plates were chosen to ensure that full penetration does not occur during the experiments. Depending upon the type of gas used and the fill pressure, projectile impact velocity varied from about 4.5 to 6 km/s.

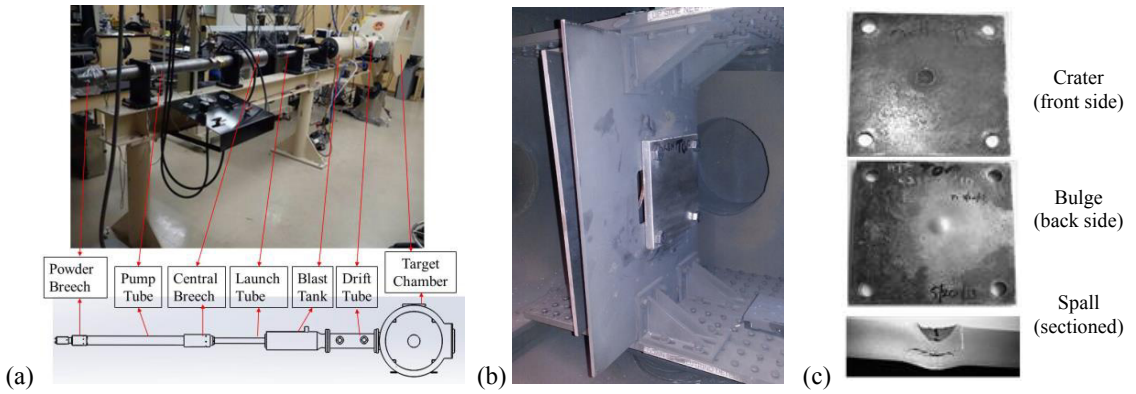

Fig. 1. (a) Two-stage gas gun in UNLV with schematic, (b) bolted target on mounting plate in target chamber, (c) target plate after impact.

2.1. MPDV

Two different types of MPDV arrangements were used in gas gun experiments using multiple optical fiber probes: 9-probe and 25-probe (Fig. 2). MPDV probes were focused on the back side of target plate to capture velocimetry data at specific points around the center of impact. Probes were spread 10 mm to 15 mm approximately in both horizontal and vertical directions on target plates. The MPDV system was triggered by the second laser in the intervalometer laser system assembly. A delay time was set in the MPDV system based on the projectile velocity to collect data from the back surface of the plate. A schematic of the data acquisition by MPDV system is shown in Fig 2c. The MPDV data were collected at a sampling rate of 10 GSa/s in all cases. Raw data are processed using a sliding fast Fourier transform (FFT) analysis to obtain the velocity profile [10].

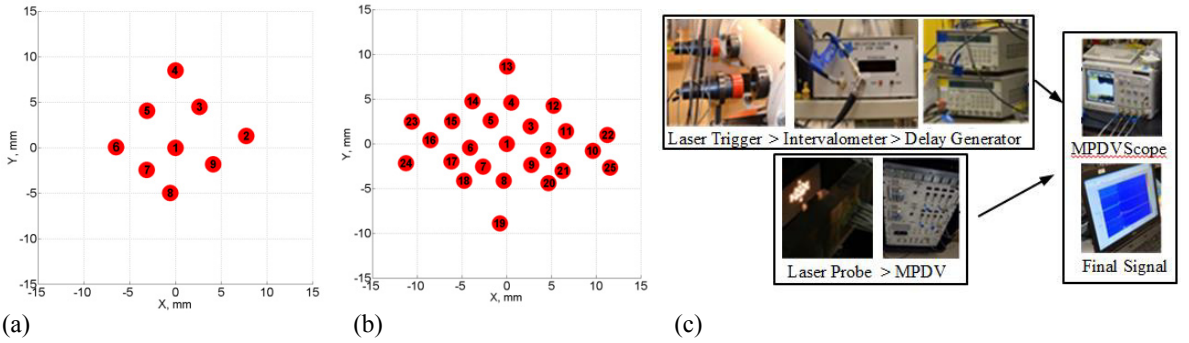

Fig. 2. Schematic of typical MPDV probes arrangement (a) 9-probe, (b) 25-probe, and (c) Schematic of MPDV data acquisition.

3. Experimental Results

3.1. Physical observation of target plate after experiments

In all experiments, the Lexan projectiles disintegrated due to the enormous stress and the heat generated upon impact with the target surface. A crater in the front side and a bulge on the back side of the target plate was created as a result of impact (Fig. 1c). Crater and bulge details of each target plate were measured. The distance between the flat rear surface of the plate and peak point of the bulge was taken to be the height of the bulge. An average value for multiple measurements of crater diameter, depth of penetration and bulge were taken as the final measurement. All the crater details and bulge dimensions are listed in Table 1. Sectioned plates showed spall due to release wave interactions. The results show that the size of spall cracks is proportional to impact velocity. Details of spall crack from some of these experiments are also listed in Table 1.

Table 1. Physical measurement of target plates after impact

Test ID	MPDV system details	Impact velocity, km/s	Crater diameter, mm	Penetration depth, mm	Bulge, mm	Spall crack details	
						Diameter, mm	Width, mm
1000-024	9 probe	5.708	17.2 ± 0.3	7.7 ± 0.3	3.1 ± 0.3	21.4 ± 0.2	1.9 ± 0.1
1000-025	9 probe	4.763	15.4 ± 0.3	6.5 ± 0.3	1.4 ± 0.1	14.5 ± 0.2	0.2 ± 0.1
1000-026	25 probe	4.823	15.1 ± 0.2	6.5 ± 0.5	1.5 ± 0.1	n/a	n/a
1000-027	25 probe	5.088	16.9 ± 0.8	7.0 ± 0.4	2.3 ± 0.2	n/a	n/a
1000-028	25 probe	5.157	15.9 ± 0.4	6.5 ± 0.5	1.7 ± 0.2	18.5 ± 0.1	0.7 ± 0.1

3.2. Free surface velocity

Typically, all MPDV experiments captured free surface velocities from target plate for 30-40μs whereas, the first 5μs contains the most important features related to the dynamic properties of the materials used. Free surface velocity profiles up to 15μs from typical 9-probe and 25-probe MPDV experiments are presented in Fig. 3. In general, A36 steel showed a two-wave structure velocity profile in compression: an elastic wave followed by a sharp plastic wave. The velocity peak for the plastic wave was proportional to the impact velocity. Velocity profiles also showed sharp elastic unloading after a second velocity peak and a spall signature in the form of a 'pullback velocity' signal within the first 5μs. In all MPDV experiments, the impact center is within ± 3.0 mm from the nearest PDV probe. Therefore, probes located closest to the impact center showed the earliest arrival of the free surface velocity signal and showed the highest peak velocities in general; but there were certain exceptions. While the exact reason of these anomalies is not yet understood completely, possible reasons may include the complex asymmetric nature of the stress wave.

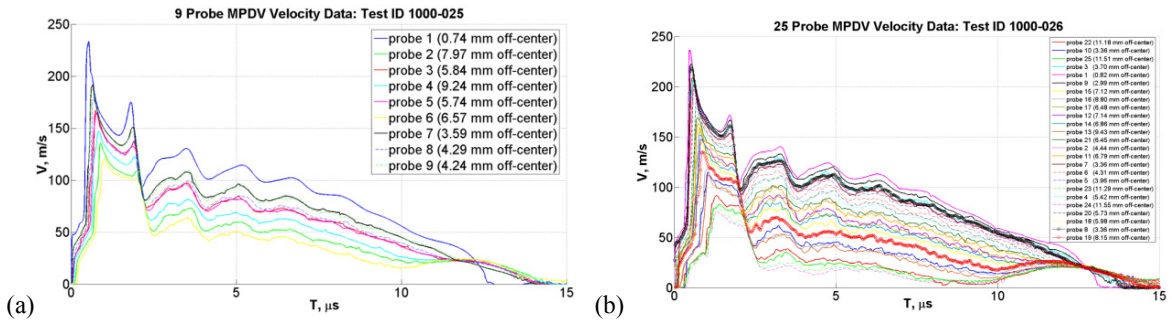

Fig. 3. Typical free surface velocity from MPDV experiment: (a) 9-probe at 4.763 km/s test (b) 25-probe at 5.157 km/s test

4. Numerical Simulations

Simulating an experiment like projectile impact on a plate at hypervelocities potentially deals with an enormous number of parameters. Under these conditions, extremely high pressure and temperature states are created that make solids behave somewhat like a fluid while retaining knowledge of their initial strength. In many cases, simulation models include many simplifications for this kind of problem, which can affect the accuracy of such simulations. In this research, the experiments were simulated using two different types of modelling approaches: Lagrangian-based smooth particle hydrodynamics (SPH) in LS-DYNA and Eulerian-based hydrocode in CTH. Obtaining a better understanding the strengths and weaknesses of both of these approaches is one of the principal motivations for this research.

4.1. Equation of State (EOS)

Materials under shock-wave loading need a numerical model that can account for the sudden pressure, temperature, internal energy, and density changes in front of shock waves. The equation of state (EOS) of a material is a general thermodynamic relation used in this type of situation. Different forms of the EOS can be used to describe dynamic behavior of different types of materials. The Mie-Grüneisen EOS model for Lexan projectiles and A36 steel were chosen to simulate all MPDV experiments in this work in both LS-DYNA and CTH. Pressure for this model [26] can be expressed as,

$$P = \frac{\rho_0 C^2 \mu[1+(1-\frac{\gamma_0}{2})\mu - \frac{a}{2}\mu^2]}{[1-(S_1-1)\mu - S_2\frac{\mu^2}{\mu+1} - S_3\frac{\mu^3}{(\mu+1)^2}]^2} + (\gamma_0 + a\mu)E \tag{1}$$

where, P is the pressure, S_1, S_2, S_3 are the coefficients of slope of shock and particle velocity curve, γ_0 is Grüneisen coefficient, a is the first order volume correction factor to γ_0, ρ is the density, C is the Hugoniot intercept of the metal, E is the absolute internal energy and $\mu = (\rho/\rho_0) - 1$. Input parameters for Lexan projectile [27] and A36 steel [28] targets are listed in Table 2.

Table 2. Gruneisen EOS parameters for Lexan and A36 steel

Material	ρ, kg/m^3	C, m/s	S_1	γ_0
Lexan	1190	1933	1.42	0.61
A36	7890	4569	1.49	2.17

4.2. Material model

The Johnson-Cook material model [29] is one of the most effective and commonly used material models for simulating compressive strength in high strain and large deformation problems [28,30–32]. In the Johnson-Cook material model of plasticity, flow stress can be expressed as Eq. (2).

$$\sigma_y = [A + B(\varepsilon^p)^n][1 + C\ln(\dot{\varepsilon}^*)][1 - (T^*)^m] \tag{2}$$

where, σ_y is the flow stress, A, B, C, n, and m are material constants, ε^p is the effective plastic strain, and $\dot{\varepsilon}^*$ is the effective total strain-rate normalized by quasi-static strain rate. T^* is the homologous temperature which can be defined as

$$T^* = \frac{T - T_r}{T_m - T_r} \tag{3}$$

where, T_r and T_m are the room temperature and melting temperature respectively. Johnson-Cook model parameters for Lexan and A36 steel are given in Table 3. No Johnson-Cook damage model was incorporated in simulation models as a pressure cut-off value (P_{min}) was used to allow spalling and damage.

Table 3. Johnson-Cook material model parameters for Lexan and A36 steel

Material	A, MPa	B, MPa	C	m	n	T_m, °K	ν
Lexan [31]	75.8	68.9	0	1.85	1.004	533	0.344
A36 [28]	286.1	500.1	0.022	0.917	0.2282	1811	0.260

4.3. Spall model

The approximate Hugoniot elastic limit (σ_{HEL}) and spall strength (σ_{spall}) of A36 steel can be calculated from free surface velocity profiles assuming a case of one dimensional localized phenomenon [33]. Although, these experiments were not uniaxial, calculating spall strength of A36 steel in this method will give an approximate value. As mentioned earlier, spall is defined as a pressure cut-off value (P_{min}) in all simulations which is a parameter of Johnson-Cook material model in LS-DYNA. Spall strength of A36 was calculated as 1.23 GPa whereas, spall strength of Lexan projectile was selected as 160 MPa [27].

4.4. SPH model in LS-DYNA

As mentioned previously, the smooth particle hydrodynamic (SPH) solver was used to simulate all these experiments in LS-DYNA. SPH is a meshless numerical technique used to model the fluid equations of motion (i.e., large distortions). Typical SPH models consist of particles which are interpolation points representing a body. Therefore, the solution of the entire system depends on an interpolation function called the 'smoothing length' [34]. In addition, parameters like particle density, bulk viscosity, and scale factors also contribute to the quality of the SPH solutions. A 2-D axisymmetric SPH model was created for both projectiles and target plates (Fig. 4a). Several SPH particle spacing arrangements were tested. SPH particle distance in the target plate was 0.05 mm while distance in the projectile was selected by matching the SPH particle mass of the projectile with SPH particle mass of the target plate. No boundary conditions were implemented as the impact is a localized phenomenon.

4.5. CTH model

CTH is an Eulerian hydrodynamics computer code developed and maintained by Sandia National Laboratories [35]. CTH simulations were also done using a 2-D axisymmetric (cylindrical) geometry (Fig. 4b). Tracer particles were placed at various target locations to collect physics information, including close to the back surface of the target where the velocimetry data are collected. Tracers were set slightly off center radially to stay away from on-axis numerical instabilities, and to match MPDV probe locations. A zone size of 0.05 x 0.05 mm was chosen for all CTH simulations after an extensive zone size study. No boundary conditions were applied in CTH model.

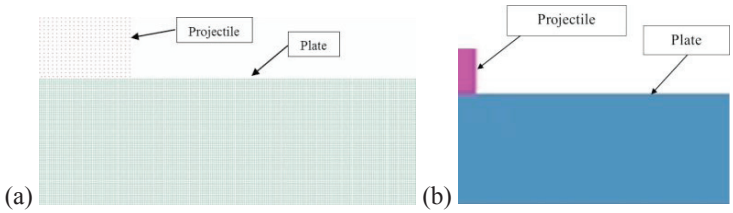

Fig. 4. Typical 2D axisymmetric model of projectile and target: (a) SPH model (zoom) in LS-DYNA (b) CTH model (zoom).

4.6. Numerical simulation results comparison

The computationally predicted deformation after impact along with the target plate back surface velocity both agree well with experimental data. Crater and bulge measurements were taken in all FEA simulations to compare with the physical measurements (Table 4).

Table 4. Typical comparison of physical measurements of crater and bulge with FEA (Test ID 1000-025)

Material	Crater diameter, mm	Difference (%)	Penetration, mm	Difference (%)	Bulge, mm	Difference (%)
Experiment	15.37	N/A	4.83	N/A	1.42	N/A
LS-DYNA (SPH)	16.20	-5.4	4.44	8.07	1.39	2.11
CTH	16.20	-5.4	4.50	6.83	1.40	1.41

To compare the free surface velocity profiles between simulation and experimental results, we narrow down the discussion to the velocity during the first 5μs after impact where most important features occur: (a) elastic precursor and Hugoniot elastic limit (HEL), (b) plastic wave (c) peak velocity (d) spall signatures. Fig. 5 shows a typical comparison of simulated velocity profiles with experimental velocity profile for a typical 9-probe MPDV experiment with an impact velocity of 4.763 km/s. Only the velocity profile close to the impact center is compared.

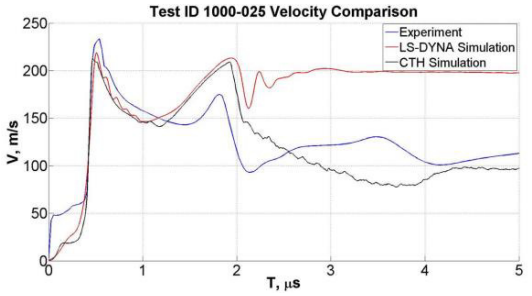

Fig. 5. Free surface velocity comparison of a typical MPDV experiment with an impact velocity of 4.763 km/s.

The results show that both LS-DYNA and CTH simulations captured the elastic precursor in a two-peak velocity profiles as observed in the experiment. But, both of these simulations showed lower HEL. For the 4.763 km/s MPDV test, the HEL calculated from free surface velocity profile is approximately 1.25±0.2 GPa. Free surface velocities from LS-DYNA and CTH showed HEL of A36 steel as 0.64 GPa and 0.57 GPa respectively. Both LS-DYNA and CTH simulation captured the sharp rise in plastic wave almost identical to the experimental results. LS-DYNA simulations registered almost same magnitude for the first peak in the experiment (6% lower velocity) but showed much higher velocity for second peak. In the case of CTH, the first peak was also lower (9% lower velocity) compare to experiment while the second peak velocity was of the same order as observed in LS-DYNA results. Both of these simulations were able to capture the pull-back velocity signal after the second peak velocity which determines spall strength of the material. However, the magnitude of the pullback velocity signal was significantly different from what was observed in the experiment, which may be due to the fact that the spall strength values used in both CTH and LS-DYNA simulations were based on one-dimensional flier plate experiments.

5. Conclusion

Gas gun experiments were performed to measure the plastic deformation of steel plates during hypervelocity impact and an MPDV system was used to measure free surface velocity during these experiments. Simulation models developed in the LS-DYNA SPH solver and the CTH hydrocode show that the physical measurements of impact cratering and bulge are in reasonable agreement with simulation results, within ±8%. Velocity profiles from both simulation models are in general agreement with the experiments capturing all the major features observed experimentally. Additional experiments and tuning of the simulation models with better physics model in terms of EOS, material models, and spall strength are needed to further refine the simulation results.

Acknowledgements

This manuscript has been authored by National Security Technologies, LLC, under Contract No. DE-AC52-06NA25946 with the U.S. Department of Energy and supported by the Site-Directed Research and Development Program. The United States Government retains and the publisher by accepting the article for publication acknowledges that the United States Government retains a non-exclusive, paid-up, irrevocable, worldwide license to publish or reproduce the published form of this manuscript, or allow others to do so, for United States Government purposes.

References

[1] Chhabildas, L. C., Knudson, M. D., 2005, Techniques to launch projectile plates to very high velocities in High-Pressure Shock Compression of Solids VIII, L. C. Chhabildas, L. Davidson,Y. Horie, Editors, Springer, Berlin Heidelberg), p. 143.
[2] Rosenberg, Z., Dekel, E., 2012, Terminal Ballistics, Springer, Berlin, Heidelberg.
[3] Merzhievskii, L. A., Titov, V. M., 1975, Perforation of Plates through High Velocity Impact, Journal of Applied Mechanics and Technical Physics 16, p. 757.
[4] Bond, J. W., Hypervelocity Impact Shock Induced Damage to Steel Armor, U.S. Army Mobility Equipment Research and Development Command, Apr. 1976.
[5] Moritoh, T., Matsuoka, S., Ogura, T., Nakamura, K. G., Kondo, K., Katayama, M., Yoshida, M., 2003. Dynamic Failure of Steel Under Hypervelocity Impact of Polycarbonate up to 9 Km/s, Journal of Applied Physics 93, p. 5983.
[6] Barker, L. M., Hollenbach, R. E., 1972. Laser Interferometer for Measuring High Velocities of Any Reflecting Surface, Journal of Applied Physics 43, p. 4669.
[7] Barker, L. M., Hollenbach, R. E., 1974, Shock Wave Study of the $\alpha \leftrightarrow \varepsilon$ Phase Transition in Iron, Journal of Applied Physics 45, p. 4872.
[8] Kuscher, G. F., Hohler, V., Stilp, A. J., 1983. High-resolution Velocity Interferometer System for Any Reflector (VISAR) Laser Interferometer Measurements of the Rear side Response of Impact Loaded Steel Plates, High Speed Photography 348, p. 508.
[9] Strand, O. T., Goosman, D. R., Martinez. C., Whitworth. T. L., Kuhlow, W. W., 2006. Compact System for High-Speed Velocimetry Using Heterodyne Techniques, Review of Scientific Instruments 77, p. 083108.
[10] Daykin, E., Perez, C., 2008. Techniques and Tools for PDV Applications: A Work in Progress, 3rd Annual PDV Workshop, Albuquerque, New Mexico.
[11] Daykin, E., Diaz, A., Gallegos, C., Perez, C., Rutkowski, A., 2010. WORK IN PROGRESS: A Multiplexed Many-Point PDV (MPDV) Techniques and Technologies, 5th Annual PDV Workshop, Ohio.
[12] Daykin, E., Burk, M., Diaz, A., Gallegos, C., Hutchins, M., Pena, M., Perez, C., Rutkowski, A., Teel, M., Theuer, K., 2011, MPDV Development, Techniques and Technologies: A Pot Load of Data, 6th Annual PDV Workshop, Livermore, California.
[13] Daykin, E., 2012, The Limits of Multiplexing, 7th Annual PDV Workshop, Albuquerque, New Mexico.
[14] Danielson, J. R., Daykin, E. P., Diaz, A. B., Doty, D. L., Frogget, B. C., Furlanetto, M. R., Gallegos, C. H., Gibo, M., Garza, A., Holtkamp, D. B., Hutchins, M. S., Perez, C., Peña, M., Romero, V. T., Shinas, M. A., Teel, M. G., Tabaka, L. J., 2014. Measurement of an Explosively Driven Hemispherical Shell using 96 Points of Optical Velocimetry, Journal of Physics Conference Series 500, p. 142008.
[15] Moro, E. A., 2014, New Developments in Photon Doppler Velocimetry, Journal of Physics Conference Series 500, p. 142023.
[16] Turley, W. D., Daykin, E., Hixson, R., LaLone, B. M., Perez, C., Stevens, G. D., Veeser, L., Ceretta, E., Gray, G. T., Rigg, P. A., Koller, D., 2014. Copper Spall Experiments with Recompression using HE (Copper Spall Soft Recovery Experiments), 8th Annual PDV Workshop, Las Vegas, NV.
[17] Zukas, J. A., 1990. High Velocity Impact Dynamics, Wiley, Michigan.
[18] Børvik, T., Langseth, M., Hopperstad, O. S., Malo, K. A., 1999. Ballistic Penetration of Steel Plates, International Journal of Impact Engineering 22, p. 855.
[19] Børvik, T., Hopperstad, O. S., Berstad, T., Langseth, M., 2001. Numerical Simulation of Plugging Failure in Ballistic Penetration, International Journal of Solids and Structures 38, p. 6241.
[20] Grady, D. E., Kipp, M. E., 1995. Experimental Measurement of Dynamic Failure and Fragmentation Properties of Metals, International Journal of Solids and Structures 32, p. 2779.
[21] Anderson, C. E., Hohler, V., Walker, J. D., Stilp, A. J., 1995. Time-Resolved Penetration Of Long Rods Into Steel Targets, International Journal of Impact Engineering 16, p. 1.
[22] Gee, D. J., 2003. Plate Perforation by Eroding Rod Projectiles, International Journal of Impact Engineering 28, p. 377.
[23] O'Daniel, J., Danielson, K., Boone, N., 2011. Modeling Fragment Simulating Projectile Penetration into Steel Plates Using Finite Elements and Meshfree Particles, Shock and Vibration 18, p. 425.
[24] Kalameh, H. A., Karamali, A., Anitescu, C., Rabczuk, T., 2012. High Velocity Impact of Metal Sphere on Thin Metallic Plate using Smooth Particle Hydrodynamics (SPH) Method, Frontiers of Structural and Civil Engineering 6, p. 101.
[25] Davis, J. R., 1998. Metals Handbook Desk Edition, ASM International.
[26] Woodruff, J. P.,1976. "KOVEC User's Manual", University of California, Lawrence Livermore National Laboratory, Livermore, California.
[27] Steinberg, D. J., 1996. Equation of State and Strength Properties of Selected Materials, Livermore, California.
[28] Seidt, J. D., Gilat, A., Klein, J. A., Leach, J. R., 2007. High Strain Rate, High Temperature Constitutive and Failure Models for EOD Impact Scenarios, SEM Annual Conference & Exposition on Experimental and Applied Mechanics, p 15.
[29] Johnson, G. R., Cook, W. H., 1983. A Constitutive Model and Data for Metals Subjected to Large Strains, High Strain Rates and High Temperatures, 7th International Symposium on Ballistics, The Hague, Netherlands, p. 541.
[30] Katayama, M., Kibe, S.,Toda, S., 1995. A Numerical Simulation Method and its Validation for Debris Impact Against the Whipple Bumper Shield, International Journal of Impact Engineering 17, p. 465.
[31] Littlewood, D. J., 2010. Simulation of dynamic fracture using peridynamics, finite element modeling, and contact, Proceedings of ASME 2010 International Mechanical Engineering Congress & Exposition , American Society of Mechanical Engineers, pp. 1-9.
[32] Elshenawy, T., Li, Q. M., 2013. Influences of Target Strength and Confinement on the Penetration Depth of An Oil Well Perforator, International Journal of Impact Engineering 54, p. 130.
[33] Mukherjee, D., Rav, A., Sur, A., Joshi, K. D., Gupta, S. C., 2014. Shock induced spall fracture in polycrystalline copper, AIP Conference Proceedings 1591, v 608, p. 608.
[34] Lacome, J. L., Espinosa, C., Gallet, C., 2002. Simulation of hypervelocity spacecrafts and Orbital Debris Collisions using Smoothed Particle Hydrodynamics in LS-DYNA, 5th Dynamics and Control of Systems and Structures in Space Conference, Cambridge, UK, p 9.
[35] Hertel, E. S., Bell, R. L., Elrick, M. G., Fransworth, A. V., Kerley, G. I., McGlaun, J. M., Petney, S. V., Silling, S. A., Taylor, P. A., Yarrington, L. , CTH: A Software Family for Multi-Dimensional Shock Physics Analysis, Sandia National Laboratories, Albuquerque, New Mexico, USA.